RESEARCH NOTE

# Aniridia due to a novel microdeletion affecting *PAX6* regulatory enhancers: Case report and review of the literature.

Andreas Syrimis[1], Nayia Nicolaou[1], Angelos Alexandrou[2], Ioannis Papaevripidou[2], Michael Nicolaou[1], Eleni Loukianou[3], Violetta Christophidou-Anastasiadou[1,4], Stavros Malas[5], Carolina Sismani[2], George A. Tanteles[1].

[1]Department of Clinical Genetics, The Cyprus Institute of Neurology and Genetics.

[2]Department of Cytogenetics and Genomics, The Cyprus Institute of Neurology and Genetics, Nicosia, Cyprus.

[3]Department of Ophthalmology, Nicosia General Hospital, Nicosia, Cyprus.

[4]Department of Clinical Genetics, Archbishop Makarios III Medical Center, Nicosia, Cyprus.

[5]Department of Developmental and Functional Genetics, The Cyprus Institute of Neurology and Genetics, Nicosia, Cyprus

**Corresponding author:** Dr. George A. Tanteles

The Cyprus Institute of Neurology and Genetics

6 International Airport Avenue, 2370 Nicosia, Cyprus

P.O.Box 23462, 1683 Nicosia, Cyprus

gtanteles@cing.ac.cy

**Running Title:** Novel 11p13 microdeletion

**Keywords:** aniridia, array-CGH, MLPA, *PAX6* deletion

## Introduction

Aniridia is a rare congenital ocular malformation that follows an autosomal dominant mode of inheritance. Most patients carry pathogenic point mutations in the paired box 6 gene (*PAX6*), but some carry deletions involving the 11p13 region, encompassing partly or completely *PAX6* or the region downstream. We identified a novel deletion, approximately 564 kb in size located about 46.5 kb downstream of *PAX6* in a family with bilateral aniridia and foveal hypoplasia using array-CGH and multiplex ligation-dependent probe amplification. We also review all of the reported deletions downstream of *PAX6* in patients with aniridia and/or other congenital malformations and define the overlapping region that leads to aniridia when deleted.

Classic aniridia (MIM #106210) is a rare congenital panocular malformation characterized by complete or partial iris hypoplasia due to heterozygous *PAX6* mutations (Nelson *et al.,* 1984; Samant *et al.,* 2016). It can be accompanied by foveal hypoplasia, strabismus and optic nerve hypoplasia, generally leading to impaired visual acuity, while late-onset manifestations may include nystagmus, glaucoma, cataract and corneal abnormalities (Valenzuela and Cline 2004). It can occur either as an isolated malformation or as part of a syndrome, such as WAGR (Wilms tumor, aniridia, genital anomalies, and mental retardation; MIM #194072), which is caused by 11p13 deletions involving *PAX6* and the adjacent *WT1* locus (Miller *et al.,* 1964). Moreover, patients with aniridia may have non-ocular sensory and neurological abnormalities, such as reduced olfaction and hearing difficulties (Hingorani *et al.,* 2012).

The prevalence of aniridia ranges from 1 in 50,000 to 1 in 100,000 livebirths (Gronskov *et al.,* 2001). Approximately two thirds of all cases are familial following an autosomal dominant mode of inheritance with complete penetrance and variable expressivity, while the remaining cases are sporadic (Gronskov et al., 2001). Heterozygous loss-of-function mutations in the paired box gene

6 gene (*PAX6*) are identified in about 94% of patients with aniridia (Robinson *et al.*, 2008). *PAX6* encodes a transcription factor that plays a crucial role in early ocular morphogenesis and development of the central nervous system. It is expressed in nasal structures, gut, pancreas, pituitary, brain and spinal cord during embryonic development. It regulates the expression of other developmental regulatory genes, cell adhesion molecules, structural proteins and also of *PAX6* itself (Simpson and Price 2002). The majority of *PAX6* pathogenic mutations, including nonsense, splice-site and frameshift mutations, cause the production of truncated transcripts resulting in haploinsufficiency. Some patients though carry deletions at 11p13, which are thought to be rare causes of aniridia, leading to partial *PAX6* deletion, complete *PAX6* deletion, or deletion of the 3' *PAX6* regulatory region leaving its entire coding region completely intact (Crolla and van Heyningen 2002). In this study, we report the identification of a novel microdeletion affecting the 3' *PAX6* regulatory region in a patient with familial aniridia and review the previously described phenotypes associated with similar microdeletions.

**Materials and Methods**

Informed consent was obtained from all family members. Bi-directional Sanger sequencing of *PAX6* was performed on an ABI 3130XL genetic analyzer (Applied Biosystems, Foster City, CA, USA). Array-CGH analysis was performed using the Cytochip ISCA array (version 1.0, BlueGnome, Cambridge, UK) with 180,000 oligos in a 4x180k format. Fluorescent ratios were calculated using the Blue Fuse Multi Software (version 4.2, BlueGnome, Cambridge, UK). MLPA was conducted using the SALSA probemix P219-B3 (MRC-Holland, Amsterdam, Netherlands). Fragment separation by capillary electrophoresis was performed on an ABI 3130xl genetic analyzer. MLPA analysis was performed using the Coffalyser.Net Software (version 1.4, MRC-Holland, Amsterdam, Netherlands). Quantitative Real Time PCR was carried out on the CFX96

Real-Time C1000 Thermal Cycler (BIO-RAD, Hercules, CA, USA) using the SsoFast Evagreen Supermix (BIO-RAD, Hercules, CA, USA). Several primers were initially designed to span the region adjacent to the deletion breakpoints at intervals of 5000 bp and then new primers were designed at 700 bp intervals. Data analysis was performed using the CFX Manager Software (BIO-RAD, Hercules, CA, USA).

**Results**

A 44-year-old female was referred to the Clinical Genetics Clinic with the diagnosis of aniridia. Her 13-year-old son was also affected. Review of her family history revealed that she was one of four siblings born to non-consanguineous parents. One of her maternal uncles was diagnosed with renal cancer at the age of 50 years. Family history was otherwise non-contributory for aniridia.

The proband was an IUGR baby born close to term with a birth weight of 1.9 kg. Bilateral aniridia was identified in early infancy. Her development was unremarkable. At the age of 35, she was incidentally diagnosed with type 2 diabetes mellitus. At the age of 38, she underwent surgery for a multinodular goiter. Histology revealed an 8mm papillary thyroid carcinoma of the isthmus (T1N0M0). She developed postural tremor at the age of 42. She also had a history of hyperlipidemia and hypovitaminosis D. On examination, her occipitofrontal circumference (ofc) was 55 cm ($50^{th}$ - $75^{th}$ centile), her weight was 79 kg ($91^{st}$ - $98^{th}$ centile) and her height was 154 cm ($2^{nd}$ - $9^{th}$ centile). She was obese with a BMI 33.3 kg/$m^2$. She was facially non-dysmorphic. She had a short neck. She had upper chest and shoulder freckling. She had a 2/6 soft systolic heart murmur. Neurology examination was non-focal. On ophthalmology evaluation, she had horizontal nystagmus and uncorrected visual acuity of 0.2 in each eye, which increased to 0.4 when corrected with myopic lenses. The intraocular pressure was 20 mmHg in the right eye and 21 mmHg in the left eye. Slit lamp examination showed near total aniridia in both eyes (Fig. 1A). The intraocular

lens in the left eye was superiorly subluxated with stretched zonules and with opacities in both eyes (cataract). Gonioscopy showed rudimentary iris tissue. Fundoscopy revealed grade 3 foveal hypoplasia, which was confirmed by optical coherence tomography (OCT) of the macula (Fig. 1B-C).

Examination of her son at the age of 13 years and 10 months revealed an ofc of 55.5 cm ($25^{th}$ - $50^{th}$ centile), a weight of 76 kg ($98^{th}$ - $99.6^{th}$ centile) and height of 166 cm ($50^{th}$ - $75^{th}$ centile). He had bilateral aniridia. He had a single left-sided irregular hyper-pigmented macule over the upper abdomen. Cardiovascular examination revealed a 2-3/6 systolic heart murmur. He was overweight with a BMI of 27.6 kg/$m^2$. Neurology examination was non-focal. Abdominal ultrasound scan was unremarkable. The son had horizontal nystagmus and uncorrected visual acuity of 0.5 in each eye, which increased to 0.9 with hypermetropic lenses. The intraocular pressure was 16 mmHg in the right eye and 17 mmHg in the left eye. Slit lamp examination showed near total aniridia in both eyes (Fig. 1A). The intraocular lens was clear without any opacities and without any lens dislocation in either eye. Fundoscopy revealed grade 1 foveal hypoplasia without any other retinal abnormality, which was confirmed with OCT of the macula (Fig. 1B-C). Abdominal ultrasound scan was unremarkable.

Bi-directional Sanger sequencing of the coding and flanking regions of *PAX6* revealed no mutations in the proband and her son. Array-CGH detected a novel heterozygous 3' deletion of approximately 577 kb in size located 37 kb downstream of *PAX6* in the 11p13 region (chr11: 31,195,401-31,772,881; Fig. 2A). This finding was confirmed by MLPA in both the proband and her son. Subsequently, qRT-PCR refined the deletion size to about 564 kb located approximately 46.5 kb downstream of *PAX6* (chr11: 31,200,388-31,764,028), encompassing the genes *DCDC1*, *DNAJC24*, *IMMP1L* and partially *ELP4*. This region also encompasses three sites that show

enrichment for the H3K27ac histone mark, which indicates the presence of potentially active enhancers. In addition one of these sites that show enrichment for the H3K27ac mark also show a high level of evolutionary conservation across 100 vertebrate species, further supporting the presence of regulatory elements (Fig. 2B).

**Discussion and Review of the Literature**

In this study, we identified a novel 564 kb deletion downstream of *PAX6* in a family with bilateral aniridia and foveal hypoplasia. Deletions of the 3' regulatory regions downstream of *PAX6* abrogate its expression leading to aniridia due to *PAX6* haploinsufficiency, a phenomenon known as position effect (Fantes *et al.,* 1995). Twenty patients with a similar deletion downstream of *PAX6* were reported in the literature to date. The phenotypes of these patients, the breakpoints as well as the genes within the deleted region are summarized in Table 1. All these patients had aniridia, except a patient with a deletion 114 kb downstream of *PAX6*, who had ocular coloboma (Guo *et al.*, 2013). A patient with a larger deletion (1.3 Mb) encompassing *MPPED2*, *DCDC5*, *DCD1*, *IMMP1L*, *DNAJC24* and *ELP4* was also reported to have autism spectrum disorder and intellectual disability in addition to aniridia (Davis *et al.,* 2008).

To further assess the prevalence of our identified deletion, we searched the DECIPHER database for patients with similar deletions downstream of *PAX6*, yielding 12 additional aniridia patients (Firth *et al.,* 2009). One of these patients was reported to have in addition congenital cataracts and nystagmus, while another one was also described to have global developmental delay. Another patient reported in DECIPHER had Rieger anomaly. Therefore, the prevalence of the 11p13 microdeletion in affected individuals seems to be high, although clinical manifestations may vary depending on the size of the deletion, the location of the breakpoints and the genes involved.

All deletions downstream of *PAX6* previously reported to cause either aniridia or other ocular malformations, including the one identified in our study, encompass a common overlapping region 244 kb in size (chr11: 31,422,424 - 31,666,340; Fig. 2B). This was previously characterized by Ansari *et al* as the 'critical region' for aniridia. This region partially encompasses *DNAJC24*, *IMMP1L*, and introns 1-7 of *ELP4* (Ansari *et al.*, 2016). A deletion including only part of the critical region was found in a patient with partial aniridia, suggesting that a partial deletion of this critical region possibly leads to a milder ocular phenotype (Fig. 2B; (Addis *et al.*, 2015).

Microdeletions including or disrupting *ELP4* were also shown to be significantly enriched in patients with a range of neurodevelopmental disorders, including autism spectrum disorder, language impairment, epilepsy, developmental delay and intellectual disability (Addis *et al.*, 2015). The phenotypes of these patients, the breakpoints as well as the genes within the deleted region are also summarized in Table 1. These microdeletions do not seem to involve the entire critical region (Fig. 2B). Only three patients carrying a deletion downstream of *PAX6* presented with aniridia (or other ocular malformations) in conjunction with a neurodevelopmental disorder (Fig. 2B) and two of these patients had a deletion involving the entire critical region. This indicates that deletions of the entire critical region (chr11: 31,422,424 - 31,666,340) cause aniridia or other ocular malformations with complete penetrance. Such deletions or smaller ones may also predispose patients to neurodevelopmental disorders with incomplete penetrance. There was no evidence of a neurodevelopmental disorder in our patients further supporting a complex genotype-phenotype relationship.

Genetic and functional studies support the presence of a *PAX6* downstream regulatory region (DRR) that is essential for *PAX6* expression in the developing ocular tissues and causes aniridia when deleted. The DRR contains six known regulatory elements: a lens-specific enhancer, an ultra-

conserved cis-regulatory enhancer called SIMO, a retina-specific enhancer located in a fragment containing HS2 and HS3 and the recently identified HS5 and HS6 elements (Kleinjan *et al.*, 2006; McBride *et al.*, 2011). These elements are located in the introns 7-9 of *ELP4*, which are upstream of the critical region, suggesting that additional regulatory elements essential for *PAX6* expression likely exist within the critical region. Deletion of the entire DRR in mice was previously shown to abrogate expression of *Pax6* in the retina, iris and the ciliary body (Kleinjan et al., 2006). This indicates that the DRR is essential for *PAX6* expression providing additional evidence to support that the underlying genetic cause of aniridia in our patients is the identified deletion, which spans the DRR and thereby abolishes *PAX6* expression in the developing eye.

In conclusion, we have identified a novel 564 kb microdeletion downstream of *PAX6* in a family with bilateral aniridia and foveal hypoplasia using both array-CGH and MLPA. The phenotype of this patient shows a great overlap with that of previously reported patients who have a similar deletion. The use of array-CGH or MLPA of *PAX6* and downstream regulatory regions is highly recommended for aniridia patients in conjunction with *PAX6* mutation screening, in order to facilitate the ascertainment of risk for other conditions, since *ELP4* and *WT1* deletions have been associated with neurodevelopmental disorders and Wilms tumor, respectively.

**Acknowledgments**

We would like to thank the family members for participating in this study.

**References**


Addis L., Ahn J. W., Dobson R., Dixit A., Ogilvie C. M., Pinto D. et al. 2015 Microdeletions of ELP4 Are Associated with Language Impairment, Autism Spectrum Disorder, and Mental Retardation. Human mutation. 36(9), 842-850.

Ansari M., Rainger J., Hanson I. M., Williamson K. A., Sharkey F., Harewood L. et al. 2016 Genetic Analysis of 'PAX6-Negative' Individuals with Aniridia or Gillespie Syndrome. PLoS One. 11(4), e0153757.

Balay L., Totten E., Okada L., Zell S., Ticho B., Israel J. et al. 2016 A familial pericentric inversion of chromosome 11 associated with a microdeletion of 163 kb and microduplication of 288 kb at 11p13 and 11q22.3 without aniridia or eye anomalies. Am J Med Genet A. 170A(1), 202-209.

Bayrakli F., Guney I., Bayri Y., Ercan-Sencicek A. G., Ceyhan D., Cankaya T. et al. 2009 A novel heterozygous deletion within the 3' region of the PAX6 gene causing isolated aniridia in a large family group. J Clin Neurosci. 16(12), 1610-1614.

Blanco-Kelly F., Palomares M., Vallespin E., Villaverde C., Martin-Arenas R., Velez-Monsalve C. et al. 2017 Improving molecular diagnosis of aniridia and WAGR syndrome using customized targeted array-based CGH. PLoS One. 12(2), e0172363.

Cheng F., Song W., Kang Y., Yu S., Yuan H. 2011 A 556 kb deletion in the downstream region of the PAX6 gene causes familial aniridia and other eye anomalies in a Chinese family. Mol Vis. 17448-455.

Crolla J. A., van Heyningen V. 2002 Frequent chromosome aberrations revealed by molecular cytogenetic studies in patients with aniridia. Am J Hum Genet. 71(5), 1138-1149.

Davis L. K., Meyer K. J., Rudd D. S., Librant A. L., Epping E. A., Sheffield V. C. et al. 2008 Pax6 3' deletion results in aniridia, autism and mental retardation. Hum Genet. 123(4), 371-378.

Fantes J., Redeker B., Breen M., Boyle S., Brown J., Fletcher J. et al. 1995 Aniridia-associated cytogenetic rearrangements suggest that a position effect may cause the mutant phenotype. Hum Mol Genet. 4(3), 415-422.

Firth H. V., Richards S. M., Bevan A. P., Clayton S., Corpas M., Rajan D. et al. 2009 DECIPHER: Database of Chromosomal Imbalance and Phenotype in Humans Using Ensembl Resources. Am J Hum Genet. 84(4), 524-533.

Gronskov K., Olsen J. H., Sand A., Pedersen W., Carlsen N., Bak Jylling A. M. et al. 2001 Population-based risk estimates of Wilms tumor in sporadic aniridia. A comprehensive mutation screening procedure of PAX6 identifies 80% of mutations in aniridia. Hum Genet. 109(1), 11-18.

Guo H., Dai L., Huang Y., Liao Q., Bai Y. 2013 A large novel deletion downstream of PAX6 gene in a Chinese family with ocular coloboma. PLoS One. 8(12), e83073.

Hingorani M., Hanson I., van Heyningen V. 2012 Aniridia. European journal of human genetics : EJHG. 20(10), 1011-1017.

Kleinjan D. A., Seawright A., Mella S., Carr C. B., Tyas D. A., Simpson T. I. et al. 2006 Long-range downstream enhancers are essential for Pax6 expression. Dev Biol. 299(2), 563-581.

Lauderdale J. D., Wilensky J. S., Oliver E. R., Walton D. S., Glaser T. 2000 3' deletions cause aniridia by preventing PAX6 gene expression. Proc Natl Acad Sci U S A. 97(25), 13755-13759.

McBride D. J., Buckle A., van Heyningen V., Kleinjan D. A. 2011 DNaseI hypersensitivity and ultraconservation reveal novel, interdependent long-range enhancers at the complex Pax6 cis-regulatory region. PLoS One. 6(12), e28616.

Miller R. W., Fraumeni J. F., Jr., Manning M. D. 1964 Association of Wilms's Tumor with Aniridia, Hemihypertrophy and Other Congenital Malformations. The New England journal of medicine. 270922-927.

Nelson L. B., Spaeth G. L., Nowinski T. S., Margo C. E., Jackson L. 1984 Aniridia. A review. Survey of ophthalmology. 28(6), 621-642.

Robinson D. O., Howarth R. J., Williamson K. A., van Heyningen V., Beal S. J., Crolla J. A. 2008 Genetic analysis of chromosome 11p13 and the PAX6 gene in a series of 125 cases referred with aniridia. Am J Med Genet A. 146A(5), 558-569.

Samant M., Chauhan B. K., Lathrop K. L., Nischal K. K. 2016 Congenital aniridia: etiology, manifestations and management. Expert Review of Ophthalmology. 11(2), 135-144.

Simpson T. I., Price D. J. 2002 Pax6; a pleiotropic player in development. BioEssays : news and reviews in molecular, cellular and developmental biology. 24(11), 1041-1051.

Valenzuela A., Cline R. A. 2004 Ocular and nonocular findings in patients with aniridia. Canadian journal of ophthalmology Journal canadien d'ophtalmologie. 39(6), 632-638.

Wawrocka A., Budny B., Debicki S., Jamsheer A., Sowinska A., Krawczynski M. R. 2012 PAX6 3' deletion in a family with aniridia. Ophthalmic Genet. 33(1), 44-48.

Zhang X., Zhang Q., Tong Y., Dai H., Zhao X., Bai F. et al. 2011 Large novel deletions detected in Chinese families with aniridia: correlation between genotype and phenotype. Mol Vis. 17548-557.

Received 23 May 2017, revised form 20 June 2017; accepted 28 August 2017

**Table 1. Deletions identified downstream of *PAX6* previously reported in literature.**

| Article | Distance from the 3' of PAX6 | Location (hg19) | Deleted genes (whole or partially) | Size | Phenotype |
|---|---|---|---|---|---|
| **Aniridia and/or other ocular malformations** | | | | | |
| (Lauderdale *et al.*, 2000) | 22.1 kb | unknown | *ELP4, IMMP1L, DNAJC24, DCDC1, DCDC5* | 975 kb | aniridia |
| | 11.6 kb | unknown | *ELP4, IMMP1L, DNAJC24, DCDC1, DCDC5* | 1105 kb | aniridia |
| (Bayrakli *et al.*, 2009) | 140 kb | chr11:31,260,340-31,666,340 | *ELP4, IMMP1L, DNAJC24, DCDC1* | 406 kb | aniridia |
| (Zhang *et al.*, 2011) | 1 kb | chr11:31, 280,628 -31,805,329 | *ELP4, IMMP1L, DNAJC24, DCDC1* | 525 kb | aniridia |
| (Cheng *et al.*, 2011) | 123 kb | chr11:31,117,827-31,683,687 | *ELP4, IMMP1L, DNAJC24, DCDC1* | 566 kb | aniridia |
| (Wawrocka *et al.*, 2012) | 85 kb | chr11:31,122,161-31,721,030 | *ELP4, IMMP1L, DNAJC24, DCDC1* | 599-652 kb | partial aniridia |
| (Guo *et al*., 2013) | 114 kb | chr11:31,010,914-31,692,238 | *ELP4, IMMP1L, DNAJC24, DCDC1, DCDC5* | 681 kb | ocular coloboma |
| (Addis *et a*l., 2015) | 96 kb | chr11:31,118,027-31,710,576 | *ELP4, IMMP1L, DNAJC24, DCDC1* | 593 kb | Rieger anomaly, aniridia |
| | 31 kb | chr11:31,172,410-31,775,457 | *ELP4, IMMP1L, DNAJC24, DCDC1* | 603 kb | aniridia |
| | 23 kb | chr:31,605,859-31,783,590 | *ELP4* | 178kb | partial aniridia |
| (Ansari *et al*., 2016) | 108 kb | chr11:30,918,066-31,698,257 | *ELP4, IMMP1L, DNAJC24, DCDC1, DCDC5* | 780 kb | aniridia |
| | 59 kb | chr11:31,010,424-31,747,424 | *ELP4, IMMP1L, DNAJC24, DCDC1, DCDC5* | 737 kb | aniridia |
| | 113 kb | chr11:31,152,003-31,693,266 | *ELP4, IMMP1L, DNAJC24, DCDC1* | 541 kb | aniridia |
| | 54 kb | chr11:31,422,424-31,751,424 | *ELP4, IMMP1L, DNAJC24* | 329 kb | aniridia |
| (Blanco-Kelly *et al.*, 2017) | 91 kb | chr11:31,147,306-31,714,853 | *ELP4, IMMP1L, DNAJC24, DCDC1* | 567 kb | aniridia |
| | 108 kb | chr11:31,186,493-31,698,208 | *ELP4, IMMP1L, DNAJC24, DCDC1* | 512 kb | aniridia |
| | 101 kb | chr11:31,083,877-31,704,548 | *ELP4, IMMP1L, DNAJC24, DCDC1* | 620 kb | aniridia |
| **Aniridia and/or other ocular malformations and neurodevelopmental disorders** | | | | | |
| (Davis *et al.*, 2008) | 4 kb | chr11:30,448,178-31,802,357 | *ELP4, IMMP1L, DNAJC24, DCDC1, DCDC5, MPPED2* | 1354 kb | aniridia, autism, moderate mental retardation |
| (Addis *et al*., 2015) | 242 kb | chr11:30,991,456-31,564,708 | *ELP4, IMMP1L, DNAJC24, DCDC1, DCDC5* | 573 kb | focal epilepsy with cortical dysplasia, mild developmental delay, adhd, neurinomas, squint, ptosis, fine motor dyspaxia |
| (Ansari *et al*., 2016) | 11 kb | chr11:31,277,819-31,795,239 | *ELP4, IMMP1L, DNAJC24, DCDC1* | 517 kb | partial aniridia, ataxia, developmental delay |

| Neurodevelopmental disorders without aniridia | | | | | |
|---|---|---|---|---|---|
| (Addis *et al*., 2015) | 260 kb | chr11:31,495,260-31,546,276 | *ELP4, IMMP1L* | 51 kb | cognitive delay, speech and language disorder, reading and spelling disorder, asd, epilepsy |
| | 181 kb | chr11:31,561,220-31,625,448 | *ELP4* | 64 kb | speech and language delay |
| | 132 kb | chr11:31,573,422-31,674,789 | *ELP4* | 101 kb | developmental delay, microcephaly |
| | 164 kb | chr11:31,584,329-31,642,325 | *ELP4* | 58 kb | language disorder, behavior problems |
| | 174 kb | chr11:31,601,768-31,632,347 | *ELP4* | 31 kb | developmental delay, hypotonia, ventriculomegaly |
| | 84 kb | chr11:31,691,270-31,722,740 | *ELP4* | 31 kb | developmental delay, speech and language disorder, microcephaly, mild cognitive delay, motor skills development disorder |
| | 59 kb | chr11:31,705,076-31,747,631 | *ELP4* | 43 kb | autism, learning difficulties |
| | 20 kb | chr11:31,760,904-31,786,914 | *ELP4* | 26 kb | moderate developmental delay, autistic traits |
| | 4 kb | chr11:31,597,322-31,802,120 | *ELP4* | 205 kb | severe intellectual disability, muscle hypotrophy, severe dysphagia,craniofacial abnormalities |
| | 31 kb | chr11:31,605,859-31,775,457 | *ELP4* | 170 kb | developmental delay, behavioral disturbances, pervasive developmental disorder |
| | 31 kb | chr11:31,625,389-31,775,457 | *ELP4* | 150 kb | behavioral and speech disorders, mild mental retardation |
| | 151 kb | chr11:31,460,506-31,655,108 | *ELP4, IMMP1L* | 195 kb | autism |
| | 199 kb | chr11:31,488,890-31,607,986 | *ELP4, IMMP1L* | 119 kb | autism |
| | 157 kb | chr11:31,518,924-31,649,475 | *ELP4, IMMP1L* | 131 kb | autism, language delay |
| | 76 kb | chr11:31,576,768-31,653,568 | *ELP4* | 77 kb | autism, coordination problems |
| | 112 kb | chr11:31,652,219-31,764,393 | *ELP4* | 112 kb | autism, language delay, mild developmental delay, motor delay |
| (Balay *et al.*, 2016) | 191 kb | chr11:31,452,082-31,615,319 | *ELP4, IMMP1L, DNAJC24* | 163 kb | autism, intellectual disability, speech abnormalities |

**Figure Legends:**

**Figure 1.** Ophthalmological findings in the index patient and her son. A) Slit-lamp photographs of the index patient (top) and her son (bottom) showing complete hypoplasia of the iris in both patients. Also lens dislocation in the left eye of the index patient is shown as well as opacities in both of her lenses. **B)** The fundus photographs of the index patient (top) and her son (bottom) showing foveal hypoplasia. **C)** The optical coherence tomography (OCT) of the macula confirming foveal hypoplasia in the index patient (left) and her son (right). L: left eye, R: right eye.

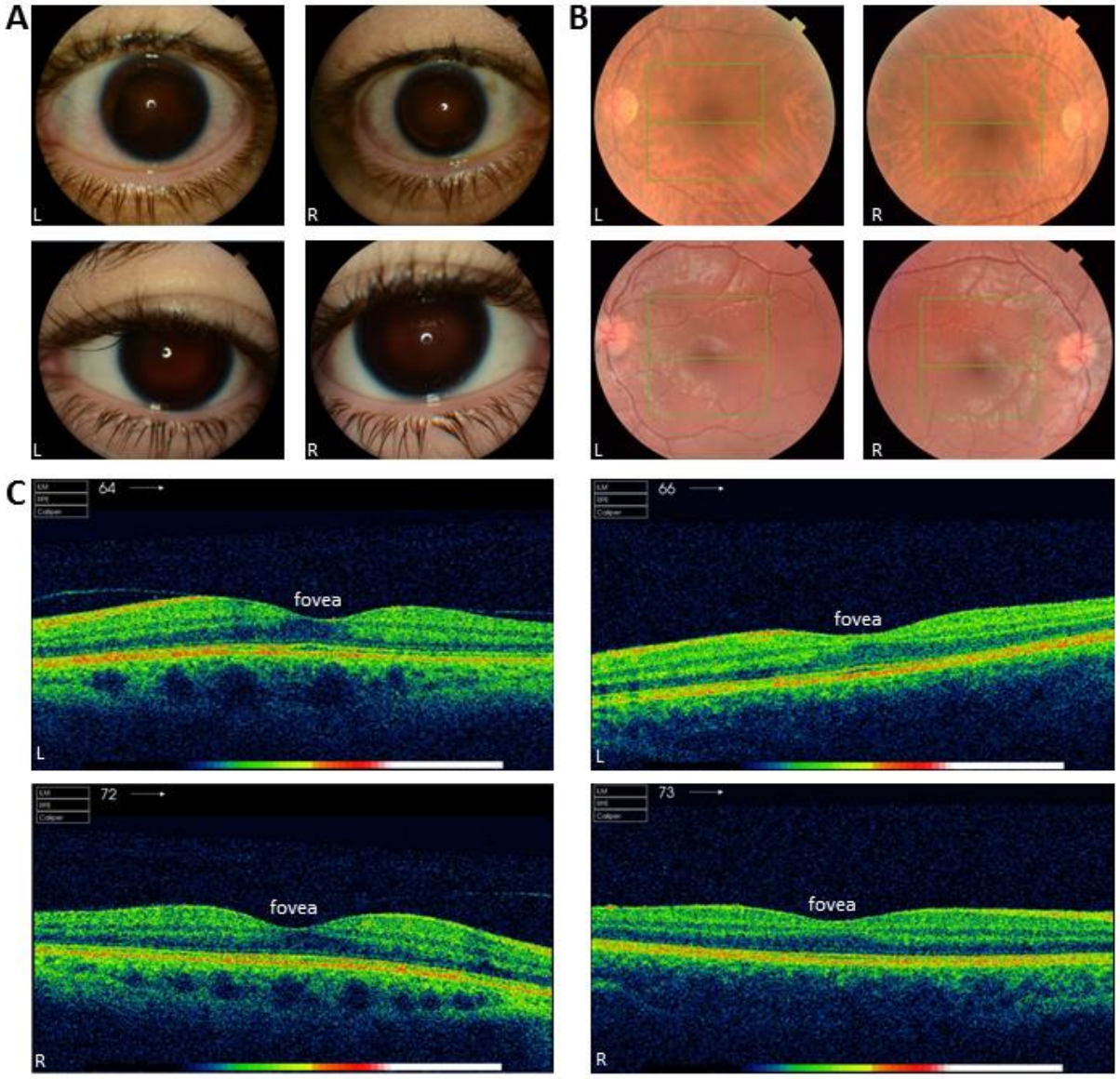
A
B
C
L
R
64
66
72
73
fovea
fovea
fovea
fovea

**Figure 2. A)** The array-CGH results showing a heterozygous deletion on chromosome 11p13 at base positions 31,195,401 and 31,722,881. This region encompasses the genes *DCDC1*, *DNAJC24*, *IMMP1L* and partially *ELP4*. The screenshot from the UCSC genome browser is showing that the deletion spans three potentially active enhancers, as indicated by the high level of enrichment of the H3K27ac histone mark (circled). These also contain DNaseI Hypersensitive sites, which also indicate the presence of regulatory regions as they tend to be DNase-sensitive, and transcription factor binding sites indicated by the black boxes. One of these regions also seems to be highly conserved as indicated by a very high level of evolutionary conservation across 100 vertebrate species. **B)** Schematic presentation of the previously reported deletions at 11p13 including the one identified in our patient. Regulatory elements SIMO, HS2-HS3, HS5 and HS6 are indicated with blue vertical boxes. Horizontal bars represent deletions that have been identified in patients with aniridia and/or other ocular malformations (red), neurodevelopmental disorders in addition to aniridia and/or other ocular malformations (blue) and neurodevelopmental disorders without ocular malformations (yellow). The vertical dashed lines indicate the overlapping region that is deleted in all patients with complete aniridia, referred to as the critical region (chr11: 31,422,424 - 31,666,340).

1*: ocular coloboma phenotype. 2*: partial aniridia phenotype.

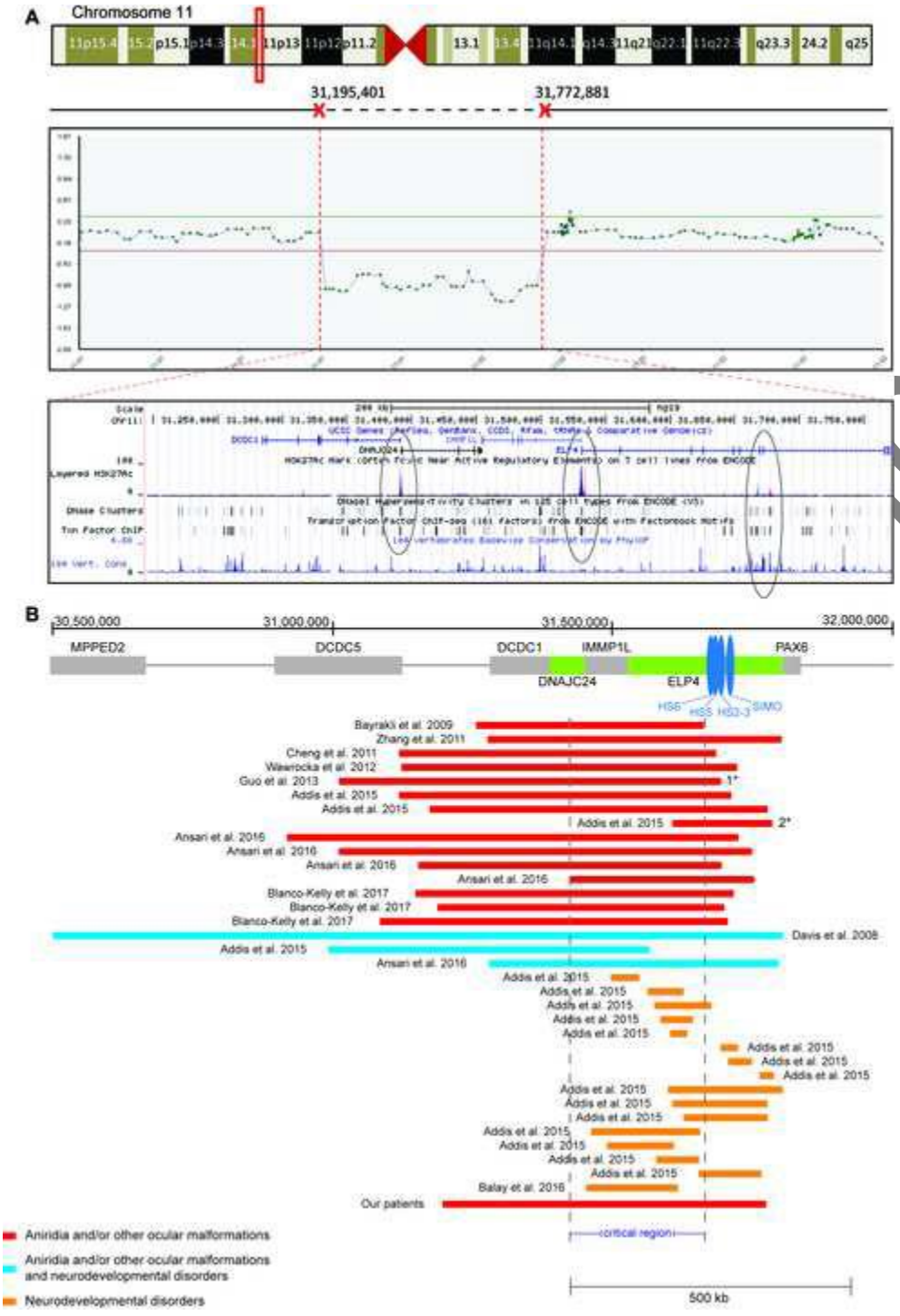
A
Chromosome 11
31,195,401
31,772,881
B
30,500,000
31,000,000
31,500,000
32,000,000
MPPED2
DCDC5
DCDC1
IMMP1L
PAX6
DNAJC24
ELP4
HS6
HS5
HS2-3
SIMO
Bayrakli et al. 2009
Zhang et al. 2011
Cheng et al. 2011
Wawrocka et al. 2012
Guo et al. 2013
1*
Addis et al. 2015
Addis et al. 2015
Addis et al. 2015
2*
Ansari et al. 2016
Ansari et al. 2016
Ansari et al. 2016
Ansari et al. 2016
Blanco-Kelly et al. 2017
Blanco-Kelly et al. 2017
Blanco-Kelly et al. 2017
Davis et al. 2008
Addis et al. 2015
Ansari et al. 2016
Addis et al. 2015
Addis et al. 2015
Addis et al. 2015
Addis et al. 2015
Addis et al. 2015
Addis et al. 2015
Addis et al. 2015
Addis et al. 2015
Addis et al. 2015
Addis et al. 2015
Addis et al. 2015
Addis et al. 2015
Addis et al. 2015
Addis et al. 2015
Addis et al. 2015
Balay et al. 2016
Our patients
critical region
500 kb
Aniridia and/or other ocular malformations
Aniridia and/or other ocular malformations and neurodevelopmental disorders
Neurodevelopmental disorders